molecules

MDPI

Article

Simple Enzyme Immobilization for Flow Chemistry? – An Assessment of Available Strategies for an Acetaldehyde Dependent Aldolase

Martin Wäscher[1], Thomas Classen[2], and Jörg Pietruszka[1,2]*

[1] Institute for Bioorganic Chemistry; Heinrich Heine University Düsseldorf; m.waescher@fz-juelich.de
[2] IBG-1: Bioorganic Chemistry; Forschungszentrum Jülich GmbH; T.Classen@fz-juelich.de
* Correspondence: j.pietruszka@fz-juelich.de; Tel.: +49(0)2461-614158

Abstract: Enzyme immobilization is an enabling technology to apply (bio-)catalysts in continuous flow systems. However, there is a plethora of immobilization methods available with individual advantages and disadvantages. Here we assessed the influence of simple and readily available methods with respect to the performance of 2-deoxy-D-ribose-5-phosphate aldolase (DERA) in continuous flow conditions. The investigated immobilization strategies cover the unspecific attachment to carrier *via* epoxides, affinity-based attachment by metal ion affinity, StrepTag™-StrepTactin™ interaction as well as covalent affinity attachment of the enzyme to a matrix tethered by the HaloTag®. The metal ion affinity-based approach outperformed the other methods in terms of immobilized activity and stability under applied conditions. As most enzymes examined today already have a HisTag for purification purposes, effective immobilization may be applied, as simple as a standard purification, if needed.

Keywords: aldolase; DERA; flow chemistry; enzyme stability; process optimization

1. Introduction

Flow chemistry is an emerging technology in organic chemistry with many advantages. For example, a reaction can be tightly controlled in terms of temperature, pressure and reaction time. Appropriate process design can compart reaction steps and therefore easily enable multistep reactions or simplify downstream processing and compound library screenings can be conducted by automation [1]. Enzymes enrich the possibilities of a chemist further, often imparting high enantio-, diastereo-, chemo-, and regioselective, respectively. Additionally, reactions can be performed under mild conditions if needed [2]. Immobilized enzymes in packed bed reactors enable the combination of these advantages. In the last decades, many ways have been described to successfully immobilize enzymes [3-5].

The 2-deoxy-D-ribose-5-phosphate aldolase (DERA) catalyzes the retro-aldol cleavage of 2-deoxy-d-ribose-5-phosphate (DRP) towards acetaldehyde and glyceradehyde-3-phosphate in deoxyribonucleic acid (DNA) degradation pathway [6,7]. It forms homodimers and is ubiquitous in nature. The DERA works in aldol direction, also. Mainly the double aldol adduct is formed this way by two subsequent aldol additions of donor acetaldehyde to a substrate and intramolecular cyclization to the hemiacetal [8]. These products can be valuable intermediates for statin side chain synthesis, for instance. Besides the industrial relevance for the double aldol products, the enantio-enriched products from single aldol reactions may be valuable intermediates, too. With a precise control of the contact time between enzyme and substrate, the mono-aldol product may be the predominant product, available for further in-line conversion to desired compounds. *Hindges et al.*

Citation: Lastname, F.; Lastname, F.; Lastname, F. Title. *Molecules* **2022**, *27*, x. https://doi.org/10.3390/xxxxx

Academic Editor: Firstname Lastname

Received: date
Accepted: date
Published: date

produced successfully a β-hydroxy carboxylic acid, a 1,3-diol, a hydroxy homoallylalcohol and a hydroxylated secondary amine in enantiopure or diastereomerically enhanced fashion, respectively, in a coupled flow/ batch process. An α,β-unsaturated aldehyde in a flow cascade could be obtained, also [9].For this study, the *E. coli* DERA C47M A95C, modified for substrate tolerance and increased structural stability was used. The C47M variation impairs the covalent inhibition by crotonaldehyde – a side-product formed from two acetaldehyde molecules [10]. The A95C variation strengthens the dimeric structure *via* an intermolecular disulfide bond [11].

The immobilization of DERA has been described as beneficial and successful in the past. The adsorption on mesoporous silica led to higher conversions by increased stability [12]. The covalent attachment of DERA on mesoporous silica *via p*-benzoquinone lead to increased substrate and temperature resistance [13]. Additional modification of matrix protein conjugate *via* amino acids increased the relative activity [14]. Immobilized DERA on carbon nanotubes showed increased stability compared to free enzyme [15]. The immobilization on polymeric thin films retains the catalysts activity [16]. Hydrophobic self-assembly of DERA thin films was achieved by poly-isopropylacrylamide conjugation [17,18]. The entrapment in alginate matrix supported by loofa sponge was investigated [19]. Even nano magnetic particles are suitable to increase substrate and temperature tolerance [20]. The entrapment in acrylic microgels is possible. However, a significant drop in activity was observed [21]. Nevertheless, a direct comparison of immobilization approaches for this enzyme could not be found.

For this study, a focus was set to simple and practical approaches. Therefore, a HaloTag®-based immobilization for specific and covalent attachment of catalyst onto carrier by ester bond was chosen as standard [22-24]. As the one-step purification and immobilization is a desired trait, the non-covalent immobilization by metal ion affinity (MIA) of His_6-tag and $His_6Gly_2Cys_2$-tag (HisNu-tag), respectively, and by StrepTag™-Strep-Tactin™ interaction were selected [25-28]. The epoxy acrylic resin *Immobead 150P* was chosen as an unselective matrix for covalent attachment [29]. To compare the immobilized DERA variants, packed bed reactors have been prepared and used for the conversion of hexanal (**1**) and acetaldehyde (**2**) to 3-hydroxyoctanal (**3**). As fixed reaction conditions have been chosen for direct comparability, side products like the aldol condensate oct-2-enal (**4**) and the cyclization product from 3,6-dihydroxy decanal (**5**), 2,4-dideoxy-3(*R*)-hydroxy-5(*R*)-pentyl-pyranoside (**6**) are expected. (see reaction scheme in Figure 1)

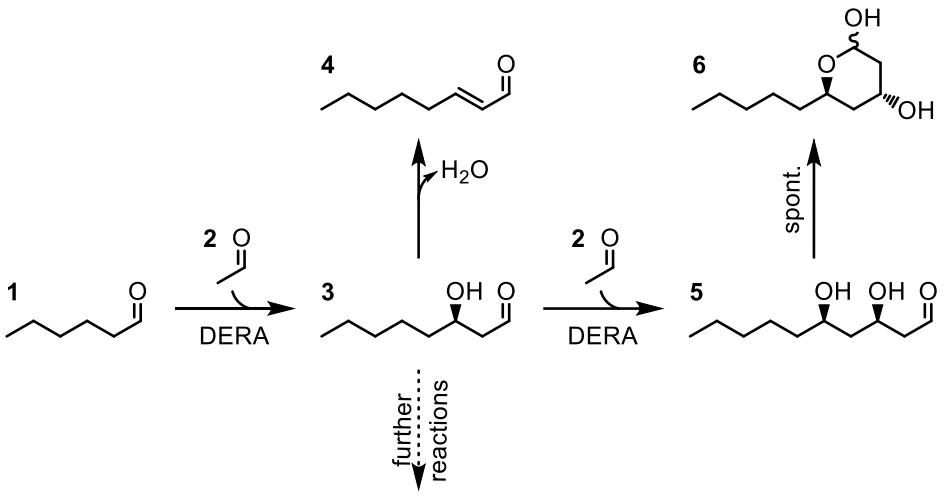

Figure 1. Reactions catalyzed by DERA, starting from hexanal (**1**). The DERA catalyses the aldol addition between hexanal (**1**) and acetaldehyde (**2**) forming (*R*)-3-hydroxy octanal (**3**) which may be used in further reactions [9]. The aldol condensation results in oct-2-enal (**4**). *(R)*-3-hydroxy-octanal (**3**) can participate in a second aldol reaction forming (*R,R*)-3,6-dihydroxy decanal (**5**) which spontaneously forms the hemiacetal 2,4-dideoxy-(*R*)-3-hydroxy-(*R*)-5-pentyl-pyranoside (**6**).

2. Results

All observations have been made with respect to the formation of (*R*)-3-hydroxy-octanal (**3**) from hexanal (**1**) and acetaldehyde (**2**) under fixed flow conditions. Therefore, the enzyme variants were immobilized as described under methods section, forming a ~350 µL packed bed reactor. The premixed reactants then are pumped through the reactor. The product stream then was extracted and analyzed *via* GC/FID (gas chromatography equipped with flame ionization detector).

2.1. Influence of tag position of enzyme for reactor

As most chosen immobilization methods rely on specific tags, the influence of the tag position for the assessed reaction was tested. For the N- and C-terminal HaloTag® variant (NHalo, CHalo) and the N- and C-terminal HisTag variant of the DERA (NHis, CHis) no difference in performance could be observed (Figure 2). As C-terminal variants could be expressed slightly better (refer Supplementary Figure 1 and Supplementary Figure 2), further studies focused on those.

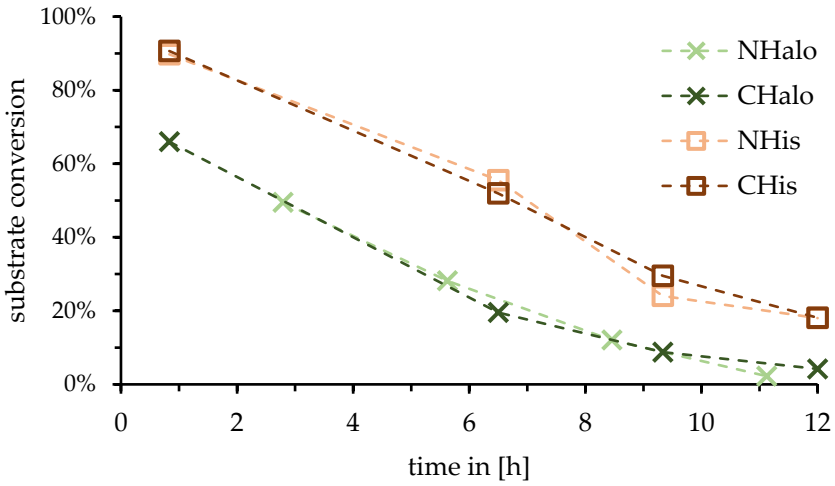

Figure 2. Change in substrate conversion over time by continuous usage for the reaction of hexanal (**1**) and acetaldehyde (**2**) towards 3-hydroxyoctanal (3) catalyzed by the DERA reactors. (hexanal (1) as observed substrate). Light-green cross: reactor with N-terminal HaloTag®-DERA (NHalo). Dark-green cross: reactor with C-terminal HaloTag®-DERA (CHalo). Light brown square: reactor with N-terminal HisTag-DERA (NHis). Dark-brown square: reactor with C-terminal HisTag-DERA (CHis). Outliers are not shown (compare Supplementary Figure 3).

2.2. Initial performance and stability of reactors

To compare the immobilization strategies, each type of reactor has been observed for three hours with respect to product stream composition. The obtained profiles can be seen in Figure 3, left. All graphs show an initial equilibration phase. This phase is between 10 min and 30 min for all reactor types, except for the Immobead-based reactor. The theoretical dead volume of the system (590 µL) partially explains this equilibration phase. For the Immobead-based reactor the time needed for reaching the plateau is 50 to 60 min.

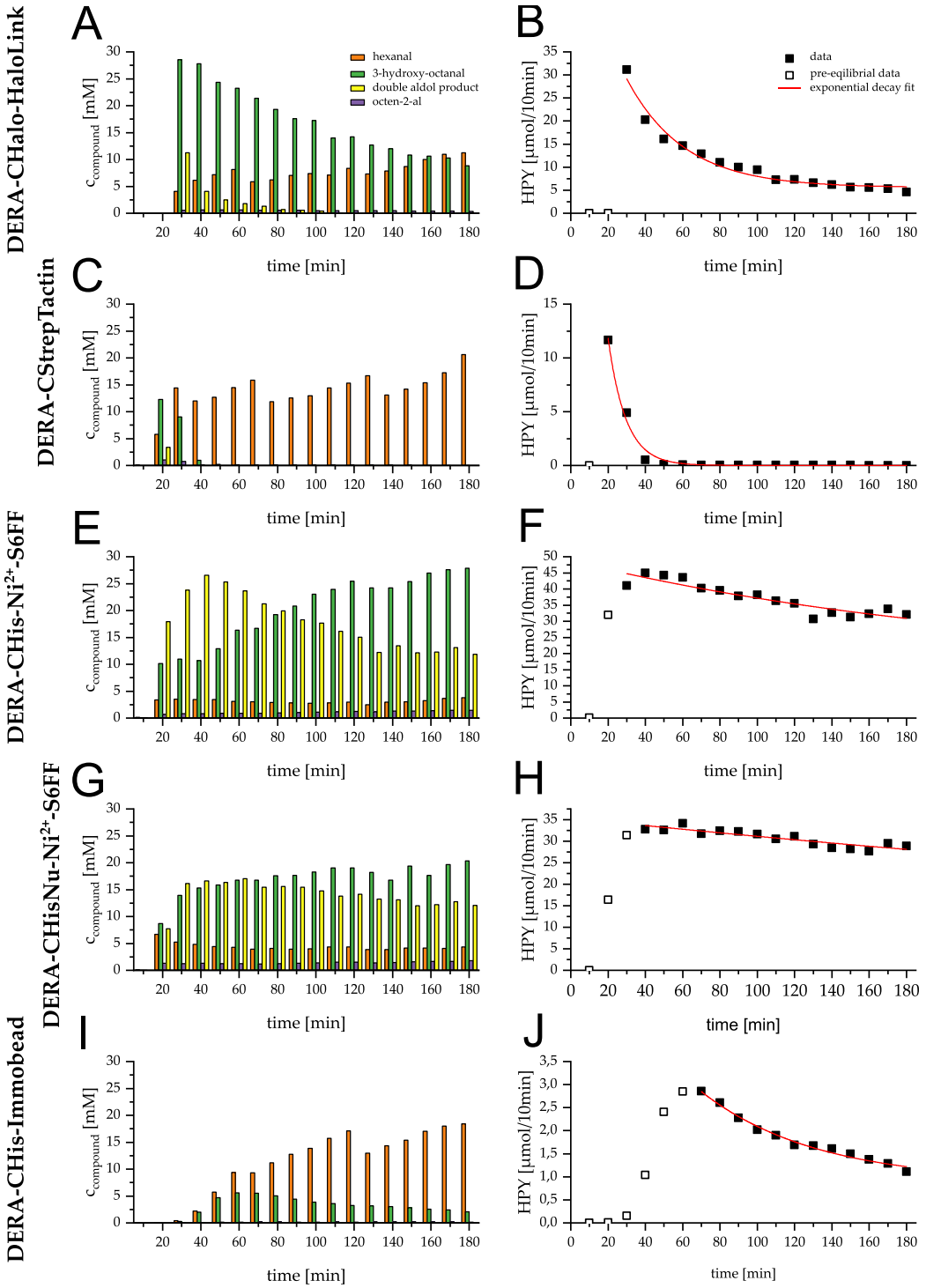

Figure 3. Left: Reactor (350 µL) performance based on different immobilizates for the reaction of 200 mM hexanal (**1**) with 600 mM acetaldehyde (**2**) in 100 mM triethanolamine (TEA) buffer pH 7 with 50 µL min^{-1}. 10 min of product stream was extracted and analyzed by GC/FID. Content of samples is shown over time: orange; hexanal (**1**) green; (*R*)-3-hydroxy-octanal (**3**) purple; octen-2-al (**4**) yellow; hemicaetale **6**. Right: Filled squares show hypothetical product yield (HPY) for 10 min timeframe of 3-hydroxy-octanal (**3**) assuming all reactor activity was used to conduct only the first aldol reaction and no aldol condensation happened. Outlined squares: fractions of the reactor's equilibration, excluded from fit. Red line shows exponential decay fit of HPY 10 min^{-1} after equilibration (for fit parameters see Supplementary Table 1). A, B: Product stream after DERA-CHalo-HaloLink® reactor. C, D: Product stream after DERA-CStrep-StrepTactin™ reactor. E, F: Product stream after DERA-CHis-Ni^{2+}-S6FF (IMAC Sepharose® 6 FastFlow) reactor. G, H: Product stream after DERA-CHisNu-Ni^{2+}-S6FF reactor. I, J: Product stream after DERA-CHis-Immobead reactor.

The reaction conditions were kept identical for direct comparison between all reactors. However, DERA reactors tend to overshoot to a second aldol reaction yielding the dideoxy sugar (**6**). As the reaction conditions are kept constant and the reaction is not optimized yet, this overshoot activity still needs to be accounted to a reactors activity. To take the side product formation into evaluation, the side product amounts are weighted rationally and summed up to a hypothetical product yield (HPY) for the samples collected over 10 min. The trend of this yield resembles an exponential decay, so a model was fitted to the data (see Figure 3, right). With those functions in hand, the half-life of the reactors could be determined. The determined parameters can be seen in Supplementary Table 1 and the calculated HPYs can be seen in Table 1.

Table 1. Derived performance indicators for DERA reactors. DERA-CHalo-Link: DeoC$_{EC}$-C47M-A95C with C-terminal HaloTag® immobilized on HaloLink®-resin. CStrep-Tactin: DeoC$_{EC}$-C47M-A95C with C-terminal StrepTag immobilized on StrepTactin™-Sepharose®. CHis-Ni-S6FF: DeoC$_{EC}$-C47M-A95C with C-terminal HisTag immobilized on IMAC Sepharose® 6 FastFlow tethered by Nickel ions. CHisNu-Ni-S6FF: DeoC$_{EC}$-C47M-A95C with C-terminal HisTag with additional Cysteins immobilized on IMAC Sepharose® 6 FastFlow tethered by nickel ions. CHis-Immobead: DeoC$_{EC}$-C47M-A95C with C-terminal HisTag immobilized on Immobead150P. Reactor size: ~350 µL. Peak yield observed directly after equilibration phase. Half-life: time until peak yield is halved, starting from peak yield time point. Exp. yield: hypothetical amount of substance produced upon reaching reactors half-life starting from peak yield time-point. Av. yield: expected hypothetical yield averaged over half-life.

	peak yield HPY/t µmol/min	half-life $\tau_{1/2}$ min	exp. yield HPY µmol	av. yield HPY/t µmol/min
DERA-CHalo-Link	2.92	30	61.5	2.07
DERA-CStrep-Tactin	1.18	7	5.7	0.85
DERA-CHis-Ni-S6FF	4.48	339	1050	3.09
DERA-CHisNu-Ni-S6FF	3.36	538	1300	2.43
DERA-CHis-Immobead	0.28	80	15.9	0.20

The metal ion affinity (MIA) based reactors started with highest hypothetical yield. 4.5 µmol min^{-1} for the MIA immobilizate originating from standard HisTag (DERA-CHis-Ni-S6FF) and 3.4 µmol min^{-1} for the variant with modified HisTag (DERA-CHisNu-Ni-S6FF). The HaloTag® based reactor showed a comparable hypothetical yield of 2.9 µmol min^{-1}, whereas the Immobead based reactor had the lowest hypothetical yield with 0.3 µmol min^{-1}. The StrepTag based reactor peaked at 1.2 µmol min^{-1}.

In terms of expected yield, the MIA-based reactors showed the highest hypothetical amount of product with 1050 µmol and 1300 µmol (DERA-CHis-Ni-S6FF and DERA-CHisNu-Ni-S6FF, respectively) upon reaching the half-life. The HaloTag®-based reactor is expected to produce ~60 µmol until its half-life. The Immobead based reactor and the StrepTag based reactor should yield 16 µmol and 6 µmol. Normalized to the reactor half-life, the HaloTag®-based and the two MIA-based reactors performed comparable with 2.1 µmol min^{-1} (DERA-CHalo-Link) 3.1 µmol min^{-1} (DERA-CHis-Ni-S6FF) and 2.4 µmol min^{-1} (DERA-CHisNu-Ni-S6FF) of hypothetical expected yield.

2.3 Time demand from harvested culture to ready reactor

Due to the demanding nature of the conducted reaction, new reactors need to be prepared constantly to maintain productivity. As the tested immobilization methods differ, the demand in time to prepare immobilizates varies, also.

In general, the reactor preparation starts with the cultivation of recombinant expression strains, including precultivation and harvesting of cells. These steps are identical for all investigated products. Therefore, the cell pellet production is not considered part of the reactor preparation. The actual preparation of a reactor involves three steps: Cell lysis, target protein isolation, and immobilization. Cell lysis was conducted by 5 min to 15 min ultrasonication treatment of resuspended pellet, a lysate separation from cell debris by centrifugation for 40 min and a short filtering through a polyethersulfone membrane, in total corresponding to one hour. The target protein isolation happens inherently during immobilization for the chosen methods except epoxy-based immobilization, where the immobilization is not guided by specific affinity and would target all proteins in solution. For this method, purification *via* immobilized metal ion affinity chromatography (IMAC) was conducted, adding two hours for this approach.

The immobilization step takes different amounts of time, depending on the applied immobilization method. For the MIA based and the StrepTag based approach 3.5 mL [~10 column volume (CV)] of filtered lysate are pumped through a packed column at 50 µL min^{-1} (roughly 0.15 CV min^{-1}). For HaloTag®-based immobilization 3.5 mL filtered lysate is pumped through a packed column at 30 µL min^{-1} according to *Döbber et al.*[30]. The Immobead 150P epoxy functionalized resin needs to be incubated with the protein solution for 24 h under gentle agitation. Regardless of immobilization method, gentle and thorough purging with buffer was done to wash out unbound and loosely bound protein. Therefore, the time demand for MIA and StrepTag based is ~2 h, for HaloTag® based ~3 h and for Immobead based immobilization ~26 h. The total time demand is visualized in Figure 4.

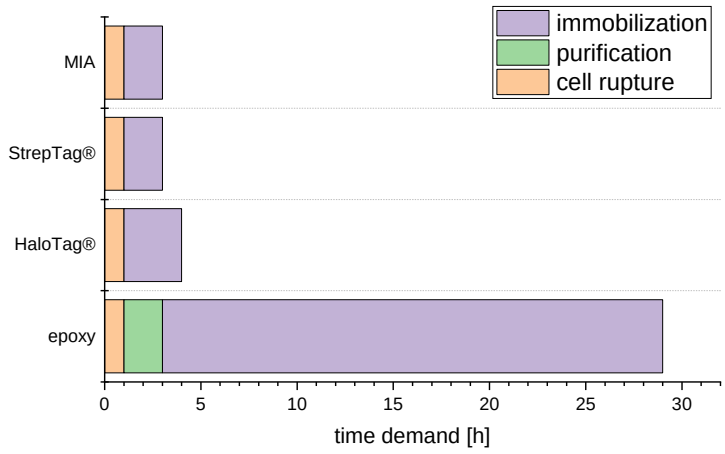

Figure 4. Time demand for reactor preparation of investigated immobilization approaches. MIA: metal ion affinity.

3. Discussion

3.1 Influence of tag position of enzyme for reactor

To investigate the influence of the tag position on the particular DERA-reactor performance, both, the Halo-Tag® and the HisTag, have been fused to the $DeoC_{EC}$-C47M-A95C N- and C-terminus, respectively. Reactors prepared with these variants showed no difference in conversion for the chosen model reaction (see Figure 2). This seemingly contradicts the work of Schulte *et al.*[31], who showed that the C-terminus of DERA significantly determines its activity. However, while in the present investigation the aldol reaction of unnatural substrate is observed, the conventional activity test utilizes the natural substrate in a retro-aldol reaction.

In any case, C-terminally modified DERA-variants were expressed slightly better than N-terminal modified variants. As no difference was observed and enough protein could be obtained, no further investigation has been conducted.

3.2 Initial performance and stability of reactors

In general, the activity of reactors drops very fast during the experiments. This can be accounted to the chosen substrate hexanal (**1**) having an amphiphilic character. Amphiphilic molecules may unfold proteins. The hydrophilic head may interact with a proteins surface. The hydrophobic tail may interacts with the protein core. This eases the unfolding of protein [32,33].

The initial equilibration phase of the reactor systems is not uniform for all reactors, although the dead volume (~ 590 µL) is the same. At a constant flow rate of 50 µL min^{-1} the theoretical equilibration time is roughly 12 min. The equilibration phase here is defined as the timeframe prior to the highest activity time point for a reactor. The equilibration phase of the DERA-CStrep-StrepTactin™ reactor is within this range. The MIA-based reactor systems and the DERA-CHalo-HaloLink® reactors equilibration phases are more in the range of 20 min to 30 min (see Figure 3). Topped by the Immobead-based reactor system with an equilibration phase of 50 min to 60 min. These differences can be explained by chromatographic interaction of the observed compounds with the respective protein carrier materials. The HaloLink® resin, the StrepTactin™ Sepharose™ and the IMAC Sepharose™ 6 FastFlow materials are based on cross-linked agarose. The hydrophilic agarose matrix in combination with aqueous buffer may lead to a small chromatographic effect. Immobeads, on the other hand, are based on methacrylamide, which is more hydrophobic. Therefore, the matrix interacts stronger with the components than with the buffer, leading to a retention. The DERA-CStrep-StrepTactin™ reactor therefore presumably shows an equilibrium phase that is close to that of a reactor without matrix effects, as this reactor type is particularly affected by rapid deactivation. The measurement here is carried out *via* the products formed, so that with a high deactivation rate the early measurement points appear apparently higher and chromatographic effects can thus hardly be detected.

In Figure 3, graph C and I show a waviness for hexanal (**1**) concentration with a 60 min period. This is an artefact due to sample handling. The sample preparation for measurements was conducted in batches of six. Therefore, the oldest sample in such batch stands already an hour in the autosamplers rack. Hexanal is somewhat volatile [1.5 kPa (25 °C) vapour pressure] [34], leading to material evaporation. To a smaller extent this is true for the desired product (*R*)-3-hydroxy-octanal (**3**), also, visible in Figure 3, graph E. The vapour pressure for (*R*)-3-hydroxy-octanal (**3**) is assumed to be smaller than the one from hexanal (**1**) due to the additional hydroxy functionality, hence this batch effect is not that prominent for this compound.

As the MIA based reactors worked relative stable within the observed period, the loss of activity shows a rather linear behaviour. To keep the comparability, exponential decay was fitted, regardless. However, as the data do not resemble an exponential decay the fit parameters inherit a high error (see Supplementary Table 1). Some models do not converge to zero activity (see Supplementary Table 1). This could be a measuring artefact or the protein is stabilized on the matrix.

Upon the tested immobilization approaches, the MIA based methods worked best for the DERA. In general, if immobilized catalyst is demanded, the MIA based immobilization is a good first choice. Not only outperformed the MIA based reactors the others in this direct comparison with respect to activity, the HisTag is commonly already fused to investigated proteins. In case, the protein-matrix conjugate is not as stable as observed here (leaching problem), the HaloTag® based immobilization is a good second choice.

3.3Time demand from harvested culture to ready reactor

Among the investigated immobilization methods, the epoxy-based immobilization takes by far the most time for reactor preparation with roughly 29 h (see Figure 4). Additionally,

the prolonged incubation for the actual oxirane opening reaction may be fatal for less stable proteins. For purified DERA just a minor loss in activity was observed. However, protection measures may need to be applied for other proteins. There is no big difference between the other methods, requiring three to four hours. Therefore, a quick preparation for a replacement reactor can be scheduled easily. From the reactor preparation time demand perspective, we conclude not to use epoxy-based immobilization methods, although forming a covalently bound catalyst.

4. Materials and Methods

4.1. Chemicals

Chemicals used in this work were commercially purchased from *Merck KGaA* and *TCI International*.

4.2. Software

OriginLab OriginPro 2019 (64-bit) v 9.6.0.172

4.3. Methods

4.3.1 Cloning of DERA mutants

The 2-deoxy-D-ribose-5-phosphate aldolase (DERA) mutants have been created over several steps by combination of restriction-ligation cloning, *Gibson* assembly, overlap extension assembly and round-the-horn mutagenesis.[39,40]. Oligonucleotides were synthesized by *Merck KGaA*. Sequence identity was checked by *GATC SupremeRun* sequencing (*eurofins genomics*).

4.3.2 Protein Production

Chemically competent *E. coli* BL21(DE3) were transformed with the respective plasmid. A colony of a transformed clone is used to inoculate a 25 mL LB_{Amp} (lysogeny broth) [41] medium overnight culture (100 μg mL^{-1} ampicillin; in 100 mL *Erlenmeyer* flask at 37 °C with 120 rpm agitation). The entire culture has been used to inoculate 1 L TB_{Amp} medium (100 μg mL^{-1} Ampicillin) [42] in 3 L *Fernbach* flask. The culture was incubated at 37 °C with 120 rpm until an optical density (OD_{600nm}) of 0.3 was reached. 100 μM isopropyl-*β*-D-thiogalactopyranosid (IPTG) was then added for induction of expression. After a 30 min cold shock on ice the culture was incubated at 25 °C with 120 rpm for 24 h. The cells were then harvested by centrifugation at 4 °C with 8200 rcf for 30 min. The DERA-containing cell pellet is stored at -20 °C until use.

4.3.3. Immobilization of DERA variants

Roughly, 1 g of DERA-containing cell pellet was resuspended with 4 mL g^{-1} in 100 mM triethanolamine (TEA) buffer pH 7. The resuspension was then ultrasonicated (*Bandelin SONOPLUS* with *SONOPLUS* KE76 cone tip, 2x - 4x 5 min, 50 % cycle, 35 % amplitude in 50 mL-reaction vessel) while chilled on ice. Lysis efficiency was determined by measuring OD_{600nm} prior and after sonication and was calculated this way:

$$lysis\ \ efficiency = 1 - \frac{OD_{post}}{OD_{pre}} \quad (1)$$

A lysis efficiency below 75 % was avoided.The crude cell extract was then centrifuged (4 °C, 7000 rcf, 40 min) and filtered with 0,2 μm polyethersulfone membrane.

For HaloTag® based reactor, an *Omnifit*® (*Diba industries*) column (3 mm Ø x 50 mm) was tightly packed with HaloLink®-Resin (*Promega*) to the total volume of ~350 μL. The resin then was washed with 10 ml deionized water, pumped with a syringe pump *kdS Legato 100* (*kdScientific*) at a flow rate of 1 mL min^{-1}. While water was pumped through, a turned on vortex was placed close to the laboratory stand to rattle out air bubbles from the column. Then, 5 mL of 100 mM TEA buffer pH 7 is flown through at 350 μL min^{-1} to equilibrate the matrix material. 3.5 mL of the filtered, DERA containing lysate are pumped though the column at 30 μL min^{-1}. This is followed by 1 mL of buffer at the same flow rate.

Together with the flown through 3.5 mL of lysate, this is considered as the flow through sample. Finally, 5 mL of buffer are applied to wash the reactor at 200 µL min^{-1}.

The protocol for metal ion affinity based (MIA) reactors and StrepTag™ based reactors is the same as for HaloTag® based. Except the flowrate for lysate loading, here 50 µL min^{-1} have been used. For MIA reactors IMAC Sepharose® 6 FastFlow (*cytiva*) was tightly packed. After washing with deionized water 1 mL of 100 mM $NiCl_2$ was pumped at 200 µL min^{-1} to charge the matrix with Ni^{2+} ions. 5 mL of deionized water at 200 µL min^{-1} are used prior to the equilibration step. For StrepTag™ based reactors the columns are packed with StrepTactin™ sepharose® (*Iba lifesciences*).

For immobilization on epoxy group carrying Immobead 150P (*ChiralVision*) purified protein is needed. Therefore, 4 g of cell pellet containing $DERA_{EC}$ DM CHis was resuspended in 16 mL 50 mm potassium phosphate (KP_i) buffer pH 7 and lysed as described above. A 5 mL HiTrap™ IMAC FF (*Cytiva*) is charged cyclic for 30 min at roughly 2 mL min^{-1} with a peristaltic P-1 pump (*Cytiva*). 10 mL of KP_i buffer are applied to wash out unbound protein. Loosely bound protein is eluted by collecting ten fractions of 5 mL with KP_i buffer containing 20 mM imidazole. The protein of interest is eluted by raising the imidazole concentration to 250 mM (also collecting ten fractions of 5 mL each). 20 mL of 1 M imidazole containing buffer is applied to elute all remaining protein. The fractions with highest specific activity are unified and concentrated two times 5 min at 5440 rcf, 4 °C with *Vivaspin*® concentrator (*Sartorius*) and desalted with PD-10 columns (*Cytiva*). 550 mg of Immobead 150P are incubated with 4.5 mL of protein preparation for 24 h under gentle agitation. Then the Immobeads are washed three times with 10 mL buffer (100 mM TEA pH 7) and filled in the *Omnifit*® column.

4.3.4 DERA activity assay

The retro aldol activity with respect to 2-deoxy-D-ribose-5-phospahte (DRP) cleavage of protein samples were measured for 25 min at 25 °C with the auxiliary proteins glycerol-3-phosphate dehydrogenase (GDH) and triosephosphate isomerase (TPI) by following the depletion of reduced nicotinamide-adenine-dinucleotide (NADH) at 340 nm with an *Infinite M1000pro* (*Tecan*) microtiter plate reader [6,43]. Per well 5 µL of sample are putted in. The assay is started by adding 195 µL of assay mix containing 188,8 µL 100 mM TEA buffer pH 7, 2 µL 40 mm DRP, 4 µL 10 mm NADH and 0,2 µL GDH/TPI-Mix (155 U GDH mg^{-1}, 1630 U TPI mg^{-1}). Protein concentration was determined by *Bradford* assay [44].

4.3.5 Initial performance flow experiment setup

200 mM hexanal **1** (above solubility, emulsion formed) and 600 mM acetaldehyde **2** are suspended in 100 mM TEA buffer pH 7 and pumped with *kdS Legato 100* (*KD Scientific*)syringe pump at 50 µL min^{-1} through a freshly prepared 350 µL reactor. Post reactor a *FC 203B* fraction collector (*GILSON*) fractionates the stream in 500 µL (10 min) samples for 3 h. The setup scheme is depicted in Figure 5.

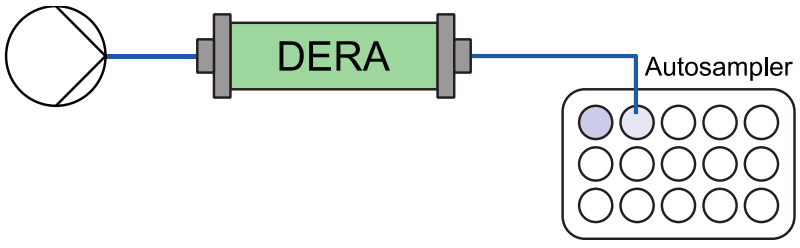

Figure 5. General flow setup. The reaction mixture containing hexanal **1** and acetaldehyde **2** in TEA puffer are pumped through a DERA containing packed bed reactor. The product stream is collected afterwards by an autosampler.

400 µL per fraction are extracted with two times 200 µL ethyl acetate with 2-phenylethanol of defined concentrations. The organic phase is collected and dried with $MgSO_4 \bullet H_2O$. The sample is then analyzed by GC/FID (gas chromatography with flame

ionization detector) [*TRACE-GC*(*ThermoQuest*), FS-Hydrodex β-3P-capillary column (*Macherey-Nagel*, 25 m 0.4 mm outer diameter, 0.25 mm inner diameter)] sample injection with MTBE (methyl-*tert*-butylether). Temperature profile: 60 °C for 5 min, 5 °C min^{-1} until 200 °C, 200 °C for 5 min. Retention times are taken from *Bisterfeld* [45]. Compound concentrations are determined as described by *de Saint Laumer et al.* [46].

4.3.6 tag position dependent performance

Reactor columns were treated with reaction mixture (200 mM hexanal and 600 mM acetaldehyde are suspended in 100 mM TEA buffer pH 7) for 12 h at 50 µL min^{-1}. A sample was collected for 40 min (2 mL). 1 mL was extracted with two times 500 µL ethyl acetate containing a defined concentration of 2-phenylethanol. The extract was dried with $MgSO_4 \cdot H_2O$ and analyzed by GC/FID [*TRACE-GC*(*ThermoQuest*), FS-Hydrodex β-3P-capillary column (*Macherey-Nagel*, 25 m 0.4 mm outer diameter, 0.25 mm inner diameter)] sample injection with MTBE (methyl-*tert*-butylether). Temperature profile: 60 °C for 5 min, 5 °C min^{-1} until 200 °C, 200 °C for 5 min.

4.3.7 Data evaluation

To calculate a hypothetical product yield, the products originating from productive conversions performed by the reactor were considered. These are the first aldol addition product -the desired product, the aldol condensate, a side product formed by condensation of desired product and the cyclized double aldol addition product, formed from a subsequent aldol addition from the desired product, catalyzed also by the reactor (refer Figure 1). As kinetic investigations of the actual catalyst – the DERA – show in general a ratio of catalytic efficiency of first aldol reaction and second aldol reaction of ~1.95, the second reaction is performed roughly half as good as the first reaction [47]. Therefore, the amount of cyclized double aldol addition product is weighted by 2.95. The exponential decay function

$$y = y_0 + A_1 e^{-\frac{x}{t_1}} \quad (2)$$

was fitted with OriginPro to the summed-up values per time batch. For the DERA-CHisNu-Ni^{2+}-S6FF data the y_0 was set to zero to reach convergence. Half-life of reactor and expected total yield per reactor are then calculated based on the model.

Supplementary Materials: The following supporting information can be downloaded at: www.mdpi.com/xxx/s1, Figure S1: title; Table S1: title; Video S1: title.

Author Contributions: Conceptualization, J.P. and T.C.; funding acquisition, J.P.; methodology, M.W.; writing—original draft preparation, M.W.; writing—review and editing, M.W., T.C., and J.P. All authors have read and agreed to the published version of the manuscript.

Funding: This research was funded by the AiF ("IGF-Vorhaben" 20341 BG).

Acknowledgments: We would like to thank A. Christina Albrecht for the review of the manuscript and Beatrix Paschold for cell cultivation.

Conflicts of Interest: The authors declare no conflict of interest.

References

1. Plutschack, M.B.; Pieber, B.; Gilmore, K.; Seeberger, P.H. The Hitchhiker's Guide to Flow Chemistry. *Chem. Rev.* **2017**, *117*, 11796-11893, doi:https://doi.org/10.1021/acs.chemrev.7b00183.
2. Sheldon, R.A.; Brady, D.; Bode, M.L. The Hitchhiker's guide to biocatalysis: recent advances in the use of enzymes in organic synthesis. *Chem. Sci.* **2020**, *11*, 2587-2605, doi:https://doi.org/10.1039/C9SC05746C.
3. Sheldon, R.A. Enzyme Immobilization: The Quest for Optimum Performance. *Adv. Synth. Catal.* **2007**, *349*, 1289-1307, doi:https://doi.org/10.1002/adsc.200700082.
4. Homaei, A.A.; Sariri, R.; Vianello, F.; Stevanato, R. Enzyme immobilization: an update. *J. Chem. Biol.* **2013**, *6*, 185-205, doi:https://doi.org/10.1007/s12154-013-0102-9.
5. Sheldon, R.A.; van Pelt, S. Enzyme immobilisation in biocatalysis: why, what and how. *Chem. Soc. Rev.* **2013**, *42*, 6223-6235, doi:https://doi.org/10.1039/C3CS60075K.
6. Racker, E. Enzymatic Synthesis and Breakdown of Desoxyribose Phosphate. *J. Biol. Chem.* **1952**, *196*, 347-365.
7. Tozzi, M.G.; Camici, M.; Mascia, L.; Sgarrella, F.; Ipata, P.L. Pentose phosphates in nucleoside interconversion and catabolism. *FEBS J.* **2006**, *273*, 1089-1101, doi:https://doi.org/10.1111/j.1742-4658.2006.05155.x.
8. Gijsen, H.J.M.; Wong, C.-H. Unprecedented Asymmetric Aldol Reactions with Three Aldehyde Substrates Catalyzed by 2-Deoxyribose-5-phosphate Aldolase. *J. Am. Chem. Soc.* **1994**, *116*, 8422-8423, doi:https://doi.org/10.1021/ja00097a082.
9. Hindges, J.; Döbber, J.; Hayes, M.R.; Classen, T.; Pohl, M.; Pietruszka, J. Covalently Immobilized 2-Deoxyribose-5-phosphate Aldolase (DERA) for Biocatalysis in Flow: Utilization of the 3-Hydroxyaldehyde Intermediate in Reaction Cascades. *ChemCatChem* **2022**, e202200390, doi:https;//doi.org/10.1002/cctc.202200390.
10. Bramski, J.; Dick, M.; Pietruszka, J.; Classen, T. Probing the acetaldehyde-sensitivity of 2-deoxy-ribose-5-phosphate aldolase (DERA) leads to resistant variants. *J. Biotechnol.* **2017**, *258*, 56-58, doi:https://doi.org/10.1016/j.jbiotec.2017.03.024.
11. Dick, M.; Weiergräber, O.H.; Classen, T.; Bisterfeld, C.; Bramski, J.; Gohlke, H.; Pietruszka, J. Trading off stability against activity in extremophilic aldolases. *Sci. Rep* **2016**, *6*, doi:https://doi.org/10.1038/srep17908.
12. Nara, T.Y.; Togashi, H.; Ono, S.; Egami, M.; Sekikawa, C.; Suzuki, Y.-h.; Masuda, I.; Ogawa, J.; Horinouchi, N.; Shimizu, S.; et al. Improvement of aldehyde tolerance and sequential aldol condensation activity of deoxyriboaldolase via immobilization on interparticle pore type mesoporous silica. *J. Mol. Catal. B: Enzym.* **2011**, *68*, 181-186, doi:https://doi.org/10.1016/j.molcatb.2010.10.008.
13. Wang, A.; Wang, M.; Wang, Q.; Chen, F.; Zhang, F.; Li, H.; Zeng, Z.; Xie, T. Stable and efficient immobilization technique of aldolase under consecutive microwave irradiation at low temperature. *Bioresour. Technol.* **2011**, *102*, 469-474, doi:https://doi.org/10.1016/j.biortech.2010.08.048.
14. Wang, A.; Gao, W.; Zhang, F.; Chen, F.; Du, F.; Yin, X. Amino acid-mediated aldolase immobilisation for enhanced catalysis and thermostability. *Bioprocess Biosyst. Eng.* **2012**, *35*, 857-863, doi:https://doi.org/10.1007/s00449-011-0670-4.
15. Subrizi, F.; Crucianelli, M.; Grossi, V.; Passacantando, M.; Botta, G.; Antiochia, R.; Saladino, R. Versatile and Efficient Immobilization of 2-Deoxyribose-5-phosphate Aldolase (DERA) on Multiwalled Carbon Nanotubes. *ACS Catal.* **2014**, *4*, 3059-3068, doi:https://doi.org/10.1021/cs500511c.
16. Reinicke, S.; Rees, H.C.; Espeel, P.; Vanparijs, N.; Bisterfeld, C.; Dick, M.; Rosencrantz, R.R.; Brezesinski, G.; de Geest, B.G.; Du Prez, F.E.; et al. Immobilization of 2-Deoxy-d-ribose-5-phosphate Aldolase in Polymeric Thin Films via the Langmuir–Schaefer Technique. *ACS Appl. Mater. Interfaces* **2017**, *9*, 8317-8326, doi:https://doi.org/10.1021/acsami.6b13632.
17. Zhang, S.; Bisterfeld, C.; Bramski, J.; Vanparijs, N.; De Geest, B.G.; Pietruszka, J.; Böker, A.; Reinicke, S. Biocatalytically Active Thin Films via Self-Assembly of 2-Deoxy-d-ribose-5-phosphate Aldolase–Poly(N-isopropylacrylamide) Conjugates. *Bioconjug. Chem.* **2018**, *29*, 104-116, doi:https://doi.org/10.1021/acs.bioconjchem.7b00645.
18. Zhang, S.; Bramski, J.; Tutus, M.; Pietruszka, J.; Böker, A.; Reinicke, S. A Biocatalytically Active Membrane Obtained from Immobilization of 2-Deoxy-d-ribose-5-phosphate Aldolase on a Porous Support. *ACS Appl. Mater. Interfaces* **2019**, *11*, 34441-34453, doi:https://doi.org/10.1021/acsami.9b12029.
19. Grabner, B.; Pokhilchuk, Y.; Gruber-Woelfler, H. DERA in Flow: Synthesis of a Statin Side Chain Precursor in Continuous Flow Employing Deoxyribose-5-Phosphate Aldolase Immobilized in Alginate-Luffa Matrix. *Catalysts* **2020**, *10*, doi:https://doi.org/10.3390/catal10010137.
20. Fei, H.; Xu, G.; Wu, J.-P.; Yang, L.-R. Improvement of the thermal stability and aldehyde tolerance of deoxyriboaldolase via immobilization on nano-magnet material. *J. Mol. Catal. B: Enzym.* **2014**, *101*, 87-91, doi:https://doi.org/10.1016/j.molcatb.2014.01.004.
21. Reinicke, S.; Fischer, T.; Bramski, J.; Pietruszka, J.; Böker, A. Biocatalytically active microgels by precipitation polymerization of N-isopropyl acrylamide in the presence of an enzyme. *RSC Adv.* **2019**, *9*, 28377-28386, doi:https://doi.org10.1039/C9RA04000E.
22. Los, G.V.; Encell, L.P.; McDougall, M.G.; Hartzell, D.D.; Karassina, N.; Zimprich, C.; Wood, M.G.; Learish, R.; Ohana, R.F.; Urh, M.; et al. HaloTag: A Novel Protein Labeling Technology for Cell Imaging and Protein Analysis. *ACS Chem. Biol.* **2008**, *3*, 373-382, doi:https://doi.org10.1021/cb800025k.
23. Encell, L.P.; Friedman Ohana, R.; Zimmerman, K.; Otto, P.; Vidugiris, G.; Wood, M.G.; Los, G.V.; McDougall, M.G.; Zimprich, C.; Karassina, N.; et al. Development of a dehalogenase-based protein fusion tag capable of rapid, selective and covalent attachment to customizable ligands. *Curr. Chem. Genomics* **2012**, *6*, 55-71, doi:https://doi.org/10.2174/1875397301206010055.

24. Döbber, J.; Pohl, M. HaloTag™: Evaluation of a covalent one-step immobilization for biocatalysis. *J. Biotechnol.* **2017**, *241*, 170-174, doi:https://doi.org/10.1016/j.jbiotec.2016.12.004.
25. Porath, J.; Carlsson, J.A.N.; Olsson, I.; Belfrage, G. Metal chelate affinity chromatography, a new approach to protein fractionation. *Nature* **1975**, *258*, 598-599, doi:https://doi.org/10.1038/258598a0.
26. Hochuli, E.; Bannwarth, W.; Döbeli, H.; Gentz, R.; Stüber, D. Genetic Approach to Facilitate Purification of Recombinant Proteins with a Novel Metal Chelate Adsorbent. *Bio/Technology* **1988**, *6*, 1321-1325, doi:https://doi.org/10.1038/nbt1188-1321.
27. Schmidt, T.G.M.; Koepke, J.; Frank, R.; Skerra, A. Molecular Interaction Between the Strep-tag Affinity Peptide and its Cognate Target, Streptavidin. *J. Mol. Biol.* **1996**, *255*, 753-766, doi:https://doi.org/10.1006/jmbi.1996.0061.
28. Skerra, A.; Schmidt, T.G.M. Applications of a peptide ligand for streptavidin: the Strep-tag. *Biomol. Eng.* **1999**, *16*, 79-86, doi:https://doi.org/10.1016/S1050-3862(99)00033-9.
29. Gennari, A.; Mobayed, F.H.; da Silva Rafael, R.; Rodrigues, R.C.; Sperotto, R.A.; Volpato, G.; Volken de Souza, C.F. Modification of Immobead 150 support for protein immobilization: Effects on the properties of immobilized Aspergillus oryzae β-galactosidase. *Biotechnol. Prog.* **2018**, *34*, 934-943, doi:https://doi.org/10.1002/btpr.2652.
30. Döbber, J.; Pohl, M.; Ley, S.V.; Musio, B. Rapid, selective and stable HaloTag-*Lb*ADH immobilization directly from crude cell extract for the continuous biocatalytic production of chiral alcohols and epoxides. *React Chem Eng* **2018**, *3*, 8-12, doi:https://doi.org/10.1039/C7RE00173H.
31. Schulte, M.; Petrović, D.; Neudecker, P.; Hartmann, R.; Pietruszka, J.; Willbold, S.; Willbold, D.; Panwalkar, V. Conformational Sampling of the Intrinsically Disordered C-Terminal Tail of DERA Is Important for Enzyme Catalysis. *ACS Catal.* **2018**, *8*, 3971-3984, doi:https://doi.org/10.1021/acscatal.7b04408.
32. O'Keefe, S.F.; Wilson, L.A.; Resurreccion, A.P.; Murphy, P.A. Determination of the binding of hexanal to soy glycinin and .beta.-conglycinin in an aqueous model system using a headspace technique. *J. Agric. Food Chem.* **1991**, *39*, 1022-1028, doi:https://doi.org/10.1021/jf00006a003.
33. Wang, K.; Arntfield, S.D. Binding of selected volatile flavour mixture to salt-extracted canola and pea proteins and effect of heat treatment on flavour binding. *Food Hydrocoll.* **2015**, *43*, 410-417, doi:https://doi.org/10.1016/j.foodhyd.2014.06.011.
34. Daubert, T.E.; Danner, R.P. *Physical and thermodynamic properties of pure chemicals: Data compilation*; Hemisphere Pub. Corp.: New York, 1989.
35. R Core Team (**2019**). R: A language and environment for statistical computing. R Foundation for Statistical Computing, Vienna, Austria. URL: https://www.R-project.org/.
36. Zeileis, A.; Grothendieck, G. zoo: S3 Infrastructure for Regular and Irregular Time Series. *Journal of Statistical Software* **2005**, *14*, 1 - 27, doi:10.18637/jss.v014.i06.
37. Hadley Wickham, Jennifer Bryan (**2019**). readxl: Read Excel Files. R package version 1.3.1. https://CRAN.R-project.org/package=readxl.
38. Jeroen Ooms (**2018**). writexl: Export Data Frames to Excel 'xlsx' Format. R package version 1.1. https://CRAN.R-project.org/package=writexl.
39. Horton, R.M.; Hunt, H.D.; Ho, S.N.; Pullen, J.K.; Pease, L.R. Engineering hybrid genes without the use of restriction enzymes: gene splicing by overlap extension. *Gene* **1989**, *77*, 61-68, doi:https://doi.org/10.1016/0378-1119(89)90359-4.
40. Gibson, D.G.; Young, L.; Chuang, R.-Y.; Venter, J.C.; Hutchison, C.A.; Smith, H.O. Enzymatic assembly of DNA molecules up to several hundred kilobases. *Nat. Meth.* **2009**, *6*, 343-345, doi:http://doi.org/10.1038/nmeth.1318.
41. Bertani, G. Studies on lysogenesis. I. The mode of phage liberation by lysogenic *Escherichia coli*. *J. Bacteriol.* **1951**, *62*, 293-300.
42. Tartoff, K.D.; Hobbs, C.A. Improved Media for Growing Plasmid and Cosmid Clones. *Bethesda Research Laboratories Focus* **1987**, *9:12*.
43. Racker, E. Spectrophotometric measurement of hexokinase and phosphohexokinase activity. *J. biol. Chem* **1947**, *167*, 843-853.
44. Bradford, M.M. A rapid and sensitive method for the quantitation of microgram quantities of protein utilizing the principle of protein-dye binding. *Anal. Biochem.* **1976**, *72*, 248-254, doi:https://doi.org/10.1016/0003-2697(76)90527-3.
45. Bisterfeld, C. Rationales Design der Acetaldehyd-abhängigen Aldolasen und deren Anwendung in der organischen Synthese. Inaugural-Dissertation, Heinrich-Heine-Universität Düsseldorf, 2016.
46. de Saint Laumer, J.-Y.; Leocata, S.; Tissot, E.; Baroux, L.; Kampf, D.M.; Merle, P.; Boschung, A.; Seyfried, M.; Chaintreau, A. Prediction of response factors for gas chromatography with flame ionization detection: Algorithm improvement, extension to silylated compounds, and application to the quantification of metabolites. *J. Sep. Sci.* **2015**, *38*, 3209-3217, doi:https://doi.org/10.1002/jssc.201500106.
47. Švarc, A.; Findrik Blažević, Z.; Vasić-Rački, Đ.; Charnock, S.J.; Vrsalović Presečki, A. A multi-enzyme strategy for the production of a highly valuable lactonized statin side-chain precursor. *Chem. Eng. Res. Des.* **2020**, *164*, 35-45, doi:https://doi.org/10.1016/j.cherd.2020.09.016.